

OPTOELECTRONIC PERFORMANCE OF TCO ON SILICON HETEROJUNCTION REAR-EMITTER SOLAR CELLS

Alexandros Cruz¹, Sebastian Neubert¹, Anna B. Morales Vilches¹, Darja Erfurt¹, Stefan Körner², Florian Ruske³, Bernd Stannowski¹, Bernd Szyszka² and Rutger Schlatmann¹

¹Helmholtz-Zentrum Berlin, PVcomB, Schwarzschildstr. 3, 12489 Berlin, Germany

²Technische Universität Berlin, Einsteinufer 25, 11087 Berlin, Germany

³Helmholtz-Zentrum Berlin, Institute for Silicon Photovoltaics, Kekuléstr. 5, 12489 Berlin, Germany

ABSTRACT: When designing silicon heterojunction (SHJ) solar cells with a rear-emitter (RE) configuration the requirements of the conductivity of the transparent conducting oxide (TCO) at the front side are relaxed due to the contribution of lateral current flow within the silicon wafer. In this study, we analyze two approaches that can be implemented to benefit from this. Firstly, the absorption of the TCO can be reduced by designing a thinner TCO layer than the single-layer anti-reflective optimum. In this case, a second anti-reflecting coating has to be deposited on top of the TCO to minimize reflection losses. Secondly, less conductive and more cost-effective materials can be used without strongly compromising the device's series resistance R_s and FF and, hence, the cell performance. To quantify the optoelectronic potential of these approaches in detail, we performed a comparative study of three different TCOs: indium tin oxide (ITO), aluminum doped zinc oxide (ZnO:Al), and hydrogenated indium oxide (IO:H) on rear-emitter SHJ solar cells. From simulations and experimental results, we conclude that, as expected, solar cells with IO:H as the front TCO reach the highest efficiency. However, low-cost and higher resistive materials such as ZnO:Al can be implemented, without having a major efficiency penalty making them, moreover, competitive to the mainstream used ITO.

1 INTRODUCTION

Silicon heterojunction (SHJ) solar cells have gained significant relevance in the past years due to their high performance, with remarkable record efficiencies of 25.1% and 26.7% for two-side contacted and all-back-contact solar cells, respectively [1]–[3]. Main drivers for these achievements have been a very good passivation of the crystalline silicon wafer and the development of highly transparent contacting materials allowing current densities of over 40 mA/cm². By using a rear-emitter (RE) configuration the requirements of the conductivity of the front transparent conductive oxide (TCO) are relaxed due to the contribution of lateral current flow in the silicon wafer [4].

In order to profit from this RE configuration, we consider two approaches that can be adopted. Firstly, the optical absorption of the TCO can be reduced if the layer is designed thinner. Moreover, less conductive materials can be implemented without compromising the series resistance of the device.

To quantify the optoelectronic potential of these approaches in detail, we performed a comparative study of three different TCOs deposited by DC sputtering: indium tin oxide (ITO), a widely used TCO on SHJ solar cells; aluminum doped zinc oxide (ZnO:Al), an attractive TCO due to its high abundance resulting in lower costs and hydrogenated indium oxide (IO:H) as a TCO with very high carrier mobility.

With a thin IO:H as front TCO layer plus a second a-SiO₂ anti reflective coating (ARC), we achieve a generated current density calculated from the external quantum efficiency of the solar cell of 40.2 mA/cm² improving the reference solar cell by 0.8 mA/cm² with respect to 39.4 mA/cm².

From electrical simulations we see that IO:H has the potential to achieve the highest efficiency of 23%. Furthermore, the higher resistive ZnO:Al can also be very competitive when implemented into RE SHJ solar cells achieving 22.6% efficiency comparable to that of

ITO with 22.7%.

2 EXPERIMENTAL DETAILS

2.1 TCO Deposition

TCO layers with thicknesses of 110±10 nm were deposited on 1.1-mm thick Corning Eagle glass in an in-line DC magnetron sputtering system from Leybold Optics (A600V7). Thicknesses were measured with a Dektak step profilometer. ITO layers were sputtered from a planar 97:3 In₂O₃:SnO₂ target, ZnO:Al from a rotatable 99:1 ZnO:Al₂O₃ target, and IO:H from a ceramic planar In₂O₃ target. ITO and ZnO:Al were deposited at a substrate temperature of about 150°C with oxygen flow ratios (O₂)=q(O₂)/q(Ar+O₂) of 2.4% and 0.48%, respectively. IO:H was deposited at room temperature (without intentional heating) with an oxygen flow ratio of 2.0% and with an introduction of water vapor resulting in 1.7x10⁻⁶ mbar partial pressure. The depositions were carried out at a base pressure of 4x10⁻⁷ mbar. IO:H samples were solid-phase crystallized by annealing in vacuum at about 180°C for 1 h.

Charge carrier mobility μ_{Hall} , and carrier concentration, N_e , were determined for TCO layers on glass by Hall measurements with an Ecopia HMS 3000 system in the van de Pauw geometry. A Perkin Elmer Lambda 1100 spectrophotometer equipped with a 150 mm integrating sphere was used for optical characterization of the TCOs. Refractive indices n and extinction coefficients k of the TCO samples, were extracted from spectrophotometer and spectroscopic ellipsometry, measurements through fitting to the Drude-Tauc-Lorenz model.

2.2 Solar Cells

For solar cells preparation, we used n-type Czochralski (CZ) silicon wafers (c-Si) with 5 Ωcm resistivity. The as-cut c-Si substrates were etched to remove the saw damage. Its surfaces were then chemically textured to obtain random pyramids with 2-4 μm average

height and <111> oriented facets. The final wafer thickness was 125 μm . After RCA cleaning and just prior to silicon deposition a dip in 1% hydrofluoric (HF) acid solution was carried out to remove native formed oxide of the surfaces. Once the substrates were conditioned, intrinsic and doped thin-film silicon layers were deposited in an AKT1600 plasma enhanced chemical vapor deposition (PECVD) tool from Applied Materials operated at 13.56 MHz plasma excitation frequency. TCO (front) and ZnO:Al-silver (back) contacts were deposited through shadow masks to define 14 4-cm² size cells, three external quantum efficiency (EQE) spots, and three transfer-length-method (TLM) spots on 5-inch wafers. A busbarless 12-finger silver grid with a total shading of $\sim 3\%$ was screen printed and cured at 210°C for 7 minutes. Finally, selected devices were coated with a-SiO₂ as a second anti-reflective layer by PECVD.

All solar cells were characterized using current voltage (I-V) measurements under an AM1.5G solar-like spectrum when illuminated and standard test conditions in a Wacom WXS-155S-L2 dual source class AAA+ sun simulator. External quantum efficiency (EQE) and electrical measurements on the TLM structures to measure TCO-silver contact resistivity were made.

3 TCO PROPERTIES

3.1 Electrical properties

ITO is a polycrystalline material that presents carrier mobilities well over 30 cm²/Vs in a broad window of carrier concentrations going from 1 to 4 $\times 10^{20}$ cm⁻³ when deposited at temperatures around 200°C [5].

The ZnO:Al presents poorer electrical properties showing mobilities between 10 and 20 cm²/Vs limited by the polycrystalline columnar growth nature of this material [18]. An important advantage for the ZnO:Al is the abundance of its components in the earth's crust in comparison to indium, positioning it as an attractive material substitute [6].

IO:H is a high-mobility TCO reaching $\mu_{\text{Hall}} > 100$ cm²/Vs.

Koida *et al.* demonstrated that this remarkable mobility is (partially) ascribed to the solid-phase crystallization leading to up to 400-nm sized grains with relaxed boundaries growing from the as-deposited amorphous material. The crystal growth is suppressed during deposition by the introduction of water (H₂O) vapor into the process chamber [7].

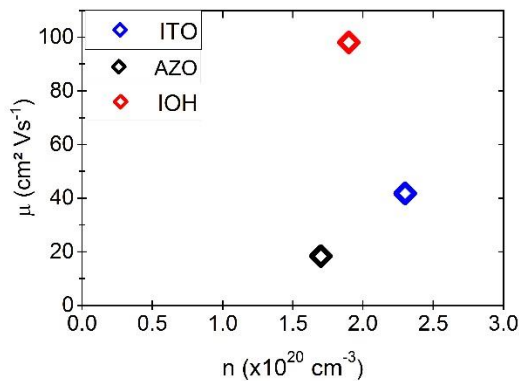


Figure 1: Hall mobility μ_{hall} vs carrier concentration N_e of selected 110±10 nm ITO, ZnO:Al and IO:H layers.

As we can see in Figure 1 the carrier concentration for the three different TCOs investigated, remains in a range of $2 \pm 0.5 \times 10^{20}$ cm⁻³, hence the difference in conductivity between them is dominated by their mobility. For the layers implemented onto devices the mobility of the ITO is 35 cm²/Vs, the ZnO:Al presents a value around 20 cm²/s and IO:H reaches values of 100 cm²/Vs. The sheet resistances (R_{sh}) of these 110±10 nm TCO layers on glass are $30 \pm 10 \Omega$ for the IO:H, $70 \pm 10 \Omega$ for the ITO and $190 \pm 20 \Omega$ for the ZnO:Al. From these reference layers, we calculate the R_{sh} of layers with different thicknesses by assuming that R_{sh} scales linearly with thickness, according to the equation $R_{\text{sh}} = \rho/t$ where ρ is the specific resistivity of the material and t is the thickness of the layer. The electrical properties of the devices, for relevant TCO thicknesses, was calculated with the Quokka2 program and will be discussed in the electrical simulations section.

3.2 Optical Properties

Figure 2 displays optical absorption spectra of the studied TCOs. We see that the differences is very subtle in the relevant range of the spectrum for the silicon absorber at the medium range and towards the near infrared region (600-1200nm), however the ZnO:Al as well as the IO:H present a slight advantage showing lower absorption than the ITO within this range. In the UV region, the IO:H shows noticeable lower absorption than the other materials. This is by combining a high optical bandgap, and a very low sub-bandgap absorption. The ZnO:Al on the other hand suffers from a higher wavelength fundamental absorption (lower band gap) positioned at 380 nm in comparison to the indium based TCOs at 350 nm.

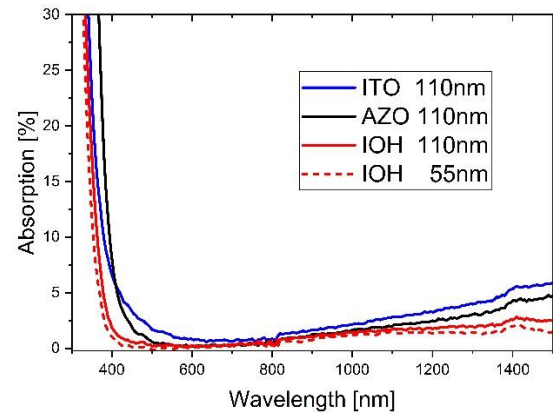


Figure 2: Optical absorption spectra of selected 110±10 nm ITO, ZnO:Al and IO:H layers on glass. An IO:H layer of 55±5 nm is presented for comparison.

By using a only 55±5-nm thick IO:H layer the absorption can be further reduced maintaining still a low enough sheet resistance of 80 Ω . This opens the possibility for a further improvement on the current density of devices. When using this thin IO:H layer a second anti-reflective layer is needed to reduce reflection losses [8]–[11]. In this case we used a-SiO₂. Reducing the layer thickness might, however, still result in higher resistive losses. In section 4.2, we quantify this effects in means of the solar cells opto-electrical performance.

4 RESULTS AND DISCUSSION

4.1 Optical performance of solar cells

To analyze the optical performance of the materials in terms of generated current, simulations with the Matlab-based one-dimensional program GenPro4 [12] were carried out for our standard SHJ solar cell material stack.

The table in Figure 3 shows the simulated current density for the investigated TCOs. We can see improvements for ZnO:Al and IO:H of 0.3, 0.4 mA/cm² over the ITO. When introducing a thinner IO:H layer with a-SiO₂ second anti-reflective coating the current increase can be further enhanced up to 0.9 mA/cm² according to the simulated values. These improvements are consistent with the absorption spectra shown for the TCOs in section 3.2.

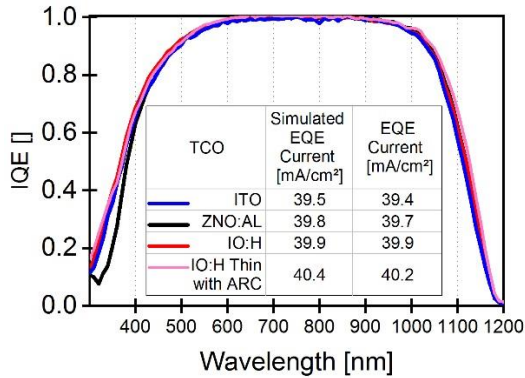


Figure 3: Internal quantum efficiency of experimental cells with different TCO (ITO, ZnO:Al, IO:H) materials with 75 nm nominal thickness. A solar cell with a thinner 35 nm IO:H layer is also presented. In the table simulated current from GenPro4 as well as calculated external quantum efficiency current densities values are presented.

To investigate the performance of the simulated solar cells on experimental devices, we processed SHJ solar cells with our standard material stack and varied the front TCO (ITO, ZnO:Al, IO:H). In Figure 3, the IQE curves for the different material combinations are shown. We see consistent improvements of the ZnO:Al and IO:H samples in comparison with the ITO reference of 0.3 and 0.5 mA/cm², respectively. We also confirm experimentally that the thinner IO:H layer with a-SiO₂ capping achieves a significant improvement of the generated current density of 0.8 mA/cm² as compared to the ITO reference and similar to the simulated values. Considering these results, we see that it is beneficial in terms of J_{sc} to implement thinner TCO layers. To quantify the performance of thinner layers for the three investigated materials further simulations were conducted to calculate the optimal TCO thicknesses for all TCOs. The resulting optimal TCO thicknesses are 40 nm for ITO and ZnO:Al and 55 nm for IO:H. For minimum reflection losses all layers must be

capped with a 90-nm thick a-SiO₂ layer. In section 4.2, we consider this optimized layer thicknesses to assess their electrical performance on devices in comparison to standard 75 nm thickness layers with a respective optimal a-SiO₂ anti reflective coating.

4.2 Electrical performance of solar cells

To simulate electrical solar cell parameters, the Quokka2 program was used [13]. For this simulation, the geometry and material properties of our standard 4 cm² solar cell as it is described in the experimental methods section was introduced. For an n-type silicon wafer the Klaassen [14] model was considered. Auger recombination was modelled after Richter [15] and radiative recombination was set to 4.73×10^{-15} cm⁻³ according to Trupke et al. [16]. For the back ZnO:Al contacting layer a $R_{sh} = 200 \Omega$ was assumed. A saturation current density of $J_0 = 15 \times 10^{-15}$ mA/cm² and a recombination current density of $J_{02} = 2.5 \times 10^{-9}$ mA/cm² were determined as the input parameters from a two-diode model fit of IV curves of one of our typical ITO solar cells. The parameters were introduced and equally distributed to the rear and the front side of the device. For the n-type front contact, the R_{sh} was varied and set to the respective TCO value. The contact resistivity ρ_c for the metal-TCO interface was derived from TLM measurements and introduced to the simulation with a value of 3 m Ω cm². For simplification the current generation was assumed to take place at the surface of the device, with a steady value at 40.7 mA/cm².

A lumped external R_s of 0.47 Ω cm² was added to account for all other R_s contributions, i. e. the grid-metal contact transport and the contact resistances at the remaining device interfaces.

Table I shows calculated R_{sh} of the TCOs at the relevant thicknesses and the simulated FF and efficiency of devices. For comparison, the best efficiency of experimental solar cells is shown too.

When analyzing the solar cells performance considering their simulated FF at a standard 75 nm TCO thickness, we can see that with a rear emitter configuration the ZnO:Al device will present a slightly lower FF than the ITO cell. However, through its improved optical properties the ZnO:Al will remain competitive showing same efficiency as the ITO of 22.5%. The IO:H device by the other side combines improved optical and electrical properties and can achieve a higher efficiency by 0.5% absolute than the other two materials. Considering the measured experimental devices we confirm that the less conductive ZnO:Al exhibits an efficiency of 22.8% comparable to the ITO with 22.5%. The IO:H cell's efficiency shows a lower value than expected being 22.4%, with reduced V_{oc} and FF. It was found that this is due to a lower pseudo Fill-Factor (pFF). We speculate that this deterioration originates from a silicon wafer passivation loss during the annealing of the sample for the

Table I: Simulated Fill-Factor FF and efficiency η for standard TCO thickness 75 nm as well as optimized layer thickness 40, 40 and 55 nm for ITO, ZnO:Al and IO:H respectively. For comparison, the best efficiencies from experimental solar cells η_{exp} is also shown.

TCO	Standard TCO thickness				Optimized TCO thickness			
	R_{sh} (Ω)	FF (%)	η (%)	η_{exp} (%)	R_{sh} (Ω)	FF (%)	η (%)	η_{exp} (%)
ITO	100	79.5	22.5	22.5	190	79.2	22.7	22.9
ZnO:Al	260	79.0	22.5	22.8	500	78.7	22.6	22.8
IO:H	60	79.7	23.0	22.4	80	79.6	23.0	22.4

IO:H solid-phase crystallization. By optimizing this process, it should be possible to exploit the full potential of this material. If we consider in Table I the optimized TCOs with reduced thickness we see a slight FF decrease due to the R_s increase as we expected. However, due to the improved optical properties of the solar cells through the thinner layers it is clear that the efficiency can be improved or in the worst case maintained equal as is the case of the IO:H. The experimental measured values confirm the slight increase or maintaining of the efficiency when designing devices with thinner TCO layers. We can also see that even for thinner TCO layers the ZnO:Al achieves comparable efficiencies as the ITO reference cell with 22.9% and 22.8%, respectively.

6. CONCLUSIONS

Through optical simulations and fabrication of experimental devices we quantitatively show the benefit that the implementation of a thinner TCO material layer in combination with a double layer anti-reflective coating with a-SiO₂ can achieve. By the introduction of such a material system in the example of a thinner IO:H layer an increase in current of 0.8 mA/cm² in comparison to an ITO standard solar cell is demonstrated.

Considering the opto-electrical performance of the solar cells we see, that the IO:H has a higher potential than the other materials increasing their efficiency by 0.5% absolute according to simulations. For the experimental devices, we do not see this performance improvement, probably due to a damage of the Si passivation during the TCO annealing process that leads to reduced values for pFF and V_{oc} .

If we implement thinner TCO layers in SHJ solar cells, simulations show that the efficiency of the devices should slightly improve or in the worst case stay the same. This is confirmed by the experimental values. We also confirm that a cost effective less conductive material in the example of ZnO:Al can be implemented into rear-emitter solar cells achieving comparable efficiencies to ITO at 22.6% and 22.7% respectively.

7. ACKNOWLEDGMENTS

The authors would like to thank Manuel Hartig Tobias Henschel, Katja Mayer-Stillrich, Jonas Pogrzeba, Holger Rhein, and Matthias Zelt for technical support. We appreciate the many valuable discussions with Dr. Martin Dimer (Von Ardenne GmbH). This work was partially funded by the German Ministry of Economic Affairs and Energy (BMWi) in the framework of the HERA project (reference #03258251).

8. REFERENCES

- [1] K. Yoshikawa *et al.*, "Silicon heterojunction solar cell with interdigitated back contacts for a photoconversion efficiency over 26%," *Nat. Energy*, vol. 2, no. 5, p. 17032, May 2017.
- [2] D. Adachi, J. L. Hernández, and K. Yamamoto, "Impact of carrier recombination on fill factor for large area heterojunction crystalline silicon solar cell with 25.1% efficiency," *Appl. Phys. Lett.*, vol. 107, no. 23, p. 233506, Dec. 2015.
- [3] M. A. Green *et al.*, "Solar cell efficiency tables (version 50)," *Prog. Photovolt. Res. Appl.*, vol. 25, no. 7, pp. 668–676, Jul. 2017.
- [4] M. Bivour, S. Schröer, M. Hermle, and S. W. Glunz, "Silicon heterojunction rear emitter solar cells: Less restrictions on the optoelectrical properties of front side TCOs," *Sol. Energy Mater. Sol. Cells*, vol. 122, pp. 120–129, Mar. 2014.
- [5] A. Valla, P. Carroy, F. Ozanne, and D. Muñoz, "Understanding the role of mobility of ITO films for silicon heterojunction solar cell applications," *Sol. Energy Mater. Sol. Cells*, vol. 157, pp. 874–880, Dec. 2016.
- [6] K. Ellmer, F. Kudella, R. Mientus, R. Schieck, and S. Fiechter, "Influence of discharge parameters on the layer properties of reactive magnetron sputtered ZnO:Al films," *Thin Solid Films*, vol. 247, no. 1, pp. 15–23, Jul. 1994.
- [7] T. Koida, M. Kondo, K. Tsutsumi, A. Sakaguchi, M. Suzuki, and H. Fujiwara, "Hydrogen-doped In₂O₃ transparent conducting oxide films prepared by solid-phase crystallization method," *J. Appl. Phys.*, vol. 107, no. 3, p. 33514, Feb. 2010.
- [8] D. Zhang *et al.*, "Design and fabrication of a SiO_x/ITO double-layer anti-reflective coating for heterojunction silicon solar cells," *Sol. Energy Mater. Sol. Cells*, vol. 117, pp. 132–138, Oktober 2013.
- [9] S. Y. Herasimenka, C. J. Tracy, V. Sharma, N. Vulic, W. J. Dauksher, and S. G. Bowden, "Surface passivation of n-type c-Si wafers by a-Si/SiO₂/SiN_x stack with <1 cm/s effective surface recombination velocity," *Appl. Phys. Lett.*, vol. 103, no. 18, p. 183903, Oct. 2013.
- [10] J. Geissbühler *et al.*, "Silicon Heterojunction Solar Cells With Copper-Plated Grid Electrodes: Status and Comparison With Silver Thick-Film Techniques," *IEEE J. Photovolt.*, vol. 4, no. 4, pp. 1055–1062, Jul. 2014.
- [11] A. B. Morales-Vilches *et al.*, "ITO-free silicon heterojunction solar cells with ZnO:Al/SiO₂ front electrodes reaching a conversion efficiency of 23 %," *IEEE JPV Submitt.*
- [12] R. Santbergen, A. H. M. Smets, and M. Zeman, "Optical model for multilayer structures with coherent, partly coherent and incoherent layers," *Opt. Express*, vol. 21, no. 102, pp. A262–A267, Mar. 2013.
- [13] A. Fell, "A Free and Fast Three-Dimensional/Two-Dimensional Solar Cell Simulator Featuring Conductive Boundary and Quasi-Neutrality Approximations," *IEEE Trans. Electron Devices*, vol. 60, no. 2, pp. 733–738, Feb. 2013.
- [14] D. B. M. Klaassen, "A unified mobility model for device simulation—I. Model equations and concentration dependence," *Solid-State Electron.*, vol. 35, no. 7, pp. 953–959, Jul. 1992.
- [15] A. Richter, S. W. Glunz, F. Werner, J. Schmidt, and A. Cuevas, "Improved quantitative description of Auger recombination in crystalline silicon," *Phys. Rev. B*, vol. 86, no. 16, p. 165202, Oct. 2012.
- [16] T. Trupke *et al.*, "Temperature dependence of the radiative recombination coefficient of intrinsic crystalline silicon," *J. Appl. Phys.*, vol. 94, no. 8, pp. 4930–4937, Sep. 2003.